Journal of Physiology (1993), **468**, *pp.* 177–200
With 11 figures
Printed in Great Britain

INHIBITORY SYNAPTIC CURRENTS IN STELLATE CELLS OF RAT CEREBELLAR SLICES

BY ISABEL LLANO AND HERSCH M. GERSCHENFELD

From the Laboratoire de Neurobiologie (CNRS URA 295), Ecole Normale Supérieure, 46 Rue d'Ulm, 75005 Paris, France

(*Received 18 March 1992*)

SUMMARY

1. In thin cerebellar slices of rats aged 14–21 days, voltage-gated currents, synaptic currents and GABA responses were studied with the tight-seal whole-cell recording technique from stellate cells (8–9 μm soma diameter) located in the outer two-thirds of the molecular layer.

2. In symmetrical Cl^- conditions, stellate cells voltage-clamped at -60 mV showed spontaneous inhibitory postsynaptic currents (IPSCs). As were the $GABA_A$ responses of the same cells, the IPSCs were blocked by bicuculline. The frequency of occurrence of IPSCs ranged from 0·2 to 1·9 events per second (21 cells). The mean amplitude of the events ranged from 61 to 226 pA (mean $\pm$ S.E.M.: 132 ± 11; n = 21).

3. The temporal course of IPSCs was characterized by a rapid rise (mean $\pm$ S.E.M. of the time to peak: $1{\cdot}1 \pm 0{\cdot}1$ ms, n = 7) and a slow decay. The decay phase was described by a double exponential function with time constants of $8{\cdot}7 \pm 0{\cdot}6$ ms, and $40{\cdot}9 \pm 3{\cdot}7$ ms respectively (means $\pm$ S.E.M.; n = 7).

4. A minor fraction (15 to 20%) of the spontaneous synaptic events recorded in control saline had a faster onset than that of the IPSCs and decayed with a rapid mono-exponential decay (time constant of 1·0–1·3 ms). These were excitatory postsynaptic currents (EPSCs) unaffected by bicuculline and blocked by the glutamate receptor antagonist 6-cyano-7-nitroquinoxaline-2,3-dione (CNQX).

5. Bath application of TTX (0·5–1 μM), which blocked voltage-gated Na^+ currents in stellate cells, induced a variable decrease in the frequency of IPSCs (mean $\pm$ S.E.M. of the frequency ratio in TTX over control: $0{\cdot}47 \pm 0{\cdot}09$; n = 12). However, the toxin had no significant effect either on the mean amplitude or on the kinetics of the IPSCs. The mean amplitude of the miniature IPSCs was 141 ± 13 pA (mean $\pm$ S.E.M.; n = 22).

6. In TTX-containing solutions, the frequency of the IPSCs was unaffected when Ca^{2+} currents were eliminated either by removal of extracellular Ca^{2+} and addition of EGTA, or by addition of Cd^{2+}. Miniature IPSCs of 200–300 pA were still observed.

7. In symmetrical Cl^- conditions, local application of GABA to stellate cells induced an inward current and an increase in membrane noise. Responses to prolonged applications of GABA showed desensitization in both whole-cell mode and somatic outside-out patches. The chord conductance estimated from recording single GABA channel events in somatic outside-out patches was 28 pS.

8. The present results suggest that in stellate cells the release of a single quantum of transmitter activates a large number of postsynaptic $GABA_A$ receptor-gated channels.

INTRODUCTION

Stellate cells are small cerebellar interneurons described originally by Ramón y Cajal (1888) in the avian cerebellum. In lower vertebrates, stellate cells are the only interneurons found in the molecular layer of the cerebellar cortex (see Ramón y Cajal, 1911; Hillman, 1969; Mugnaini, 1972). In mammals, two types of interneurons, basket cells and stellate cells, are present in this region of the cerebellar cortex. Basket cells are found almost exclusively in the lower third of the molecular layer, while stellate cells are located in the outer two-thirds of the molecular layer (Ramón y Cajal, 1911; Palkovits, Magyar & Szentágothai, 1971; Chan-Palay & Palay, 1972; Palay & Chan-Palay, 1974). In the development of the rat cerebellum, stellate cells are already in place by postnatal day 7, they become differentiated by postnatal days 11–12 and their dendrites are fully developed on postnatal day 15 (Altmann, 1972*a*, *b*, 1976).

Eccles, Llinás & Sasaki (1966*a*, *b*) showed that stellate cells play an important role as interneurons in a collateral inhibitory pathway from parallel fibres to Purkinje cells (see Llinás, 1969). Stellate cells are GABAergic; they take up ^{3}H-labelled GABA (Hökfelt & Ljungdahl, 1972; Schon & Iversen, 1972) and it has been shown immunohistochemically that they contain glutamic acid decarboxylase, the enzyme that synthesizes GABA from glutamate (see Oertel, Mugnaini, Schemechel, Tappaz & Kopin, 1982).

In spite of this precise knowledge of their morphology, development, cytochemistry and physiological role, there have been no studies of the electrophysiological features of the stellate cells to date. Using tight-seal whole-cell recording methods, we analysed the voltage-gated currents, the synaptic currents and the GABA-induced responses of stellate cells of cerebellar slices from young rats. In this paper, we describe in detail the amplitude distributions and kinetic characteristics of the spontaneous inhibitory synaptic currents recorded from stellate cells in a control extracellular medium (IPSCs) and after elimination of all regenerative electrical activity in the slice, miniature IPSCs (mIPSCs). Estimates of the single channel conductance of $GABA_A$ channels are provided from measurements of elementary currents in outside-out patches from stellate cell somata.

Some of these results were presented in a preliminary form at the Cambridge Meeting of the European Neuroscience Association (Llano & Gerschenfeld, 1991).

METHODS

Preparation of cerebellar slices

The basic procedure for obtaining and maintaining cerebellar slices followed the methods described by Llinás & Sugimori (1980) with slight modifications (Edwards, Konnerth, Sakmann & Takahashi, 1989; Llano, Marty, Armstrong & Konnerth, 1991*b*). Rats aged 14–21 days were killed by decapitation after cervical dislocation, and slices (160 μm thick) were cut from the cerebellar vermis in the sagittal plane (parallel to the plane of Purkinje cells). Slices were kept at 34 °C in oxygenated HCO_3/H_2PO_4 buffered saline (BBS, see composition below) for 1–6 h before being transferred to the experimental set up.

Patch-clamp recordings

Patch-clamp recordings were made from stellate cells in cerebellar slices visualized through an upright binocular microscope equipped with Nomarski optics (Axioscope, Carl Zeiss, 7082 Oberknochen, Germany) the eyepiece and water immersion objective giving a $\times 400$ magnification. These conditions allowed easy resolution of the various layers and cell types within the cerebellar cortex. Stellate cells were selected as cells having a soma diameter of 8–9 μm, located within the outer two-thirds of the molecular layer. Recordings from stellate cells were obtained without prior cleaning of the neuron surface. During recording, the slices were maintained at room temperature (20–22 °C). They were perfused at a rate of 1·5–2 ml/min with BBS which contained (mM): 125 NaCl, 2·5 KCl, 2 $CaCl_2$, 1 $MgCl_2$, 1·25 NaH_2PO_4, 26 $NaHCO_3$ and 25 glucose. This solution was continuously bubbled with a mixture of 95% O_2 and 5% CO_2, the solution pH being thus kept at 7·4.

The tight-seal whole-cell recording technique (Hamill, Marty, Neher, Sakmann & Sigworth, 1981) was used in most experiments presented in this paper. Recording pipettes were pulled from borosilicate glass, fire-polished and coated with beeswax. When filled with internal saline they had resistances of 3·5–4·5 MΩ. All the recordings of voltage-activated inward currents, GABA responses and spontaneous synaptic currents were performed using Cs^+-containing internal solutions, which had the following composition (mM): 150 CsCl, 2 $MgCl_2$, 0·1 $CaCl_2$, 1 CsEGTA, 10 CsHepes, 0·4 NaGTP and 4 NaATP (pH = 7·3). Recordings of outward currents were performed using a K^+ containing solution; its composition was (mM): 150 KCl, 2 $MgCl_2$, 0·1 $CaCl_2$ 1 K EGTA, 10 K Hepes, 0·4 NaGTP and 4 NaATP (pH = 7·3). Membrane currents were recorded with a patch-clamp amplifier (Axoclamp 200, Axon Instruments Inc., USA). Unless otherwise specified, the holding potentials were kept at −60 mV. The whole-cell capacitance cancellation circuit of the amplifier was used to compensate the initial portion of the capacitance transient elicited by 10 mV hyperpolarizing pulses, and to estimate the value of the series resistance. The dial settings of the cancellation circuit ranged from 5 to 8 pF. Typical values for the series resistance were 10–12 MΩ. The series resistance compensation of the amplifier was set to between 60% and 100%.

For analysis of γ-aminobutyric acid (GABA)-gated channels, outside-out patches were obtained from stellate cell somata. Borosilicate pipettes with resistances of 7–10 MΩ were used for these experiments. They were filled with the standard CsCl solution described above.

Drug application

Local application of GABA was performed using the U-tube method of Krishtal & Pidoplichko (1980), as described in Llano, Leresche & Marty (1991*a*). Pharmacological agents were applied dissolved either in the bathing solution or in the solution flowing through the U-tube. In the case of bath applications, given the perfusion rate (1·5–2 ml/min) and the volume (700 μl) of the chamber, exchange of the external solution could be achieved within one minute. Local applications through the U-tube will be called puff-applications in the remainder of the text.

The glutamate antagonist 6-cyano-7-nitroquinoxaline-2,3-dione (CNQX) and the $GABA_A$ receptor antagonist bicuculline methachloride were purchased from Tocris Neuramin Ltd, Bristol, UK. All other chemicals used were purchased from Sigma Chemical Co., France.

TTX was dissolved in 0·5% acetic acid at a concentration of 200 μM. CNQX and bicuculline methachloride were dissolved in distilled water at a concentration of 1 mM. The pH of the CNQX solution was adjusted to pH 7·0 with NaOH. The stock solutions were stored frozen, and the final concentrations were obtained by diluting the stock solutions in the saline, just before their use in the experiments.

Data acquisition and analysis

Voltage-activated membrane currents were filtered with an 8-pole Bessel filter (Frequency Devices, USA) set at a corner frequency of 5 kHz, digitized on line at a rate of 50 μs per point and stored on disk for subsequent analysis. Spontaneous synaptic currents were filtered at 2–3 kHz and acquired continuously during the experiment on video tape. They were later digitized at sampling rates of 100–200 μs per point and transferred to computer disk for analysis. In three cells (e.g. Fig. 7) the analysis was performed on data filtered at 5 kHz and sampled at 50 μs per point. No significant difference in the amplitude values or in the parameters characterizing the time course of the IPSCs was found using the higher sampling rate.

Spontaneous synaptic currents were detected and processed using two software packages. The

first one, written in our laboratory, detects an event if the difference between successive data points exceeds a given threshold (6–8 pA for the data presented in this paper). The program will then search the data points which follow, until it finds a point going back towards the baseline level. The value preceding this data point will be subtracted from the baseline value and kept as the event amplitude. Each event was visually inspected before being accepted. The resulting list of event amplitudes was used for the construction of amplitude histograms. The program also sums the amplitudes of detected events within user defined time bins, in order to assess the level of spontaneous synaptic activity under different experimental conditions. A different program, loaned by Dr S. F. Traynelis (Salk Institute of Biological Studies, La Jolla, CA, USA) was used for the analysis of the time course of synaptic events. This program also produces a list of the amplitudes of detected (visually inspected) events. No difference in the amplitude distributions yielded by the two programs was found. For analysis of kinetic parameters, events having inflections in the rising phase were rejected. The rise time was calculated as the difference in time between the first deflection from the baseline current and the time at the peak of the event. The routine used for fitting model exponentials to the decay phase of spontaneous events is based on a simplex algorithm.

When reference is made to the characteristics of synaptic events analysed from a given cell (amplitude, frequency or kinetic parameters), statistical values are presented as a mean ± standard deviation. For presentation of average values from several cells, mean values of the variable in question have been pooled and the statistical values are presented as means ± standard errors of the mean.

Analysis of single channel events was performed using a commercially available program package (Fetchan and Pstat; Axon Instruments, USA). Data were filtered at 2 kHz and sampled at 50–100 μs per point. Running data point histograms were first constructed to obtain an initial estimate of the amplitude of the single channel events. Reconstruction of events was then performed through the automatic detection routine, setting the detection threshold at a value corresponding to 50 % of the estimate of single channel current yielded by the raw data histogram. Events of duration shorter than 500 μs were excluded.

RESULTS

Identification of stellate cells

The present study is based on whole-cell recordings from forty-one cells which were selected on the basis of their size (8–9 μm soma diameter) and location (in the outer two-thirds of the molecular layer of the cerebellar cortex). As the patch-clamp pipette came into contact with the cell body and seal formation proceeded, extracellular currents due to the spontaneous firing of action potentials were always observed. In the whole-cell recording configuration, these cells had input resistances of 2–7 GΩ at −80 mV when dialysed with KCl solutions. All of them were endowed with voltage-dependent membrane conductances and showed spontaneous synaptic currents.

The recording of spontaneous action potentials before breaking into the cells and of voltage-gated and spontaneous synaptic currents in the whole-cell configuration supported the identification of these cells as neurons. When Lucifer Yellow was included in the pipette solution, the cells filled with the dye presented multiple dendrites of irregular diameter and a multi-branching axon typical of stellate cells as described by Golgi staining (Chan-Palay & Palay, 1972). On some occasions, whole-cell recordings obtained from cells in the same area showed neither voltage-activated nor spontaneous synaptic currents. No action potentials were observed extracellularly when patch-clamping these cells. We interpreted these as being either glial cells or immature granule cells caught in their displacement towards the granular layer. They were not further studied.

Voltage-dependent ionic currents of stellate cells

Figure 1*A* illustrates typical voltage-gated membrane currents recorded from a stellate cell with a CsCl-containing patch pipette, as the membrane potential was stepped from a holding level of −60 mV to the indicated values for 40 ms. For depolarizations to voltages higher than −50 mV the inward currents activated rapidly upon pulse onset and decayed to less than 20% of the peak value within

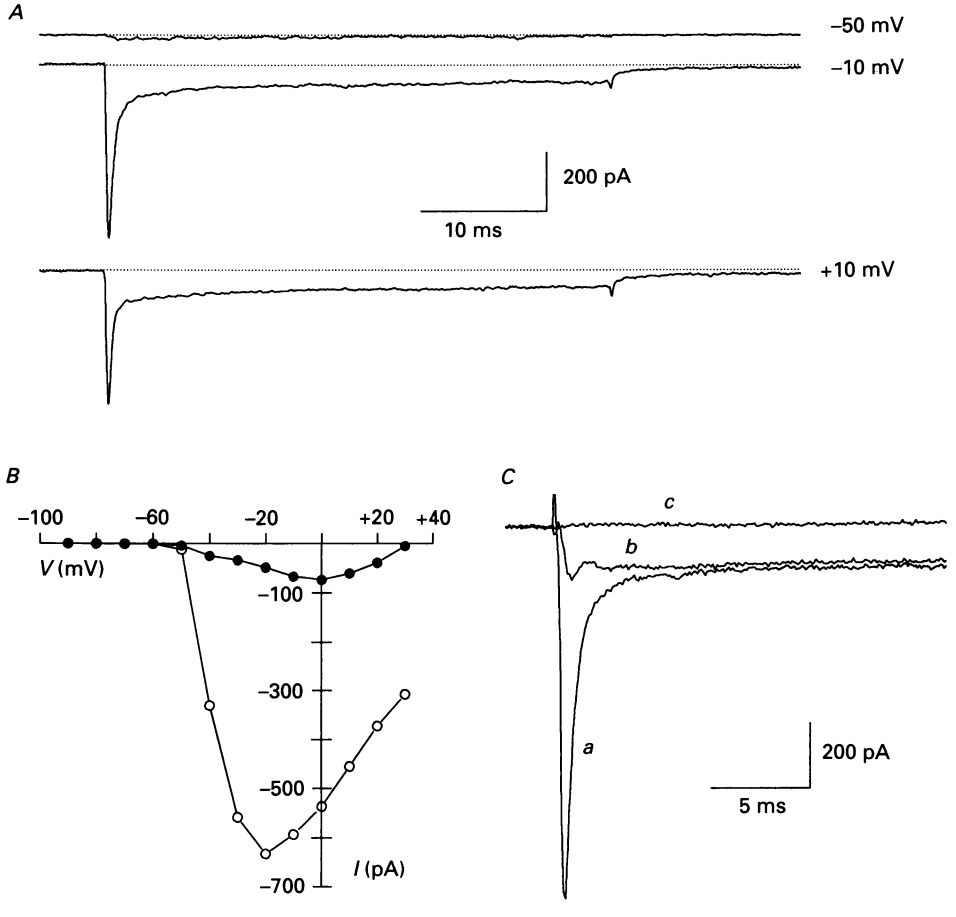

Fig. 1. Voltage-gated inward currents in cerebellar stellate cells. *A*, whole-cell currents elicited by 40 ms depolarizing steps from a holding potential of −60 mV to the values given at the right of each trace. External solution, BBS; internal solution, CsCl. *B*, current–voltage relation for the cell presented in *A*. ○, peak inward current, ● current measured 35 ms after pulse onset. *C*, currents elicited by 40 ms depolarizations to −20 mV from a holding potential of −70 mV in another stellate cell. The slice was bathed initially in BBS (trace *a*). Trace *b* was recorded 2·5 min after addition of 100 nM TTX to the external solution. Trace *c* was recorded 3 min after changing the bath solution to a Ca^{2+}-free saline, with 200 μM EGTA, 2 mM Mg^{2+} and 1 μM TTX. Internal solution, CsCl. In both *A* and *C*, leak currents and capacitative transients have been subtracted from the raw current records using appropriately scaled averaged current responses to 5 steps of −30 mV.

2 ms. The sustained inward currents were followed by inward current tails upon return to the holding potential. The current–voltage relations for the peak value of the inward current (open circles) and for the value of the current at 35 ms after pulse onset (filled circles) are presented in Fig. 1*B*. Figure 1*C* shows the membrane currents elicited in another stellate cell by depolarizations to −20 mV from a holding potential of −70 mV in control saline (*a*) and 2·5 minutes after adding 100 nM TTX to the perfusing solution (*b*). Under these conditions, the initial, inactivating component of the inward current was decreased to 9% of its control value. The sustained current was not affected. In twelve cells in which the block of inward current by TTX was examined, a small transient inward current remained at TTX concentrations of 0·5 to 1 μM (see inset in Fig. 5*A* for an example). The TTX-insensitive component of the transient inward current, as well as the sustained inward current were abolished by removal of external Ca^{2+} and addition of EGTA to the bath solution (trace *c*, Fig. 1*C*; see also inset in Fig. 5*A*). The presence of $CdCl_2$ (200 μM) in the saline was equally effective in blocking the TTX-insensitive inward current. It can thus be concluded that most of the transient inward current corresponds to the activation of voltage-gated Na^+ channels while the small transient, TTX-insensitive inward current as well as the sustained component of the inward current originate from the activation of voltage-gated Ca^{2+} channels. Evidence of clamp failure in the recordings of inward currents was frequently observed, especially when the depolarizing steps were applied from lower membrane potentials (−80 to −90 mV), resulting in larger peak Na^+ currents due to removal of inactivation.

Figure 2*A* shows the membrane currents recorded in a cell dialysed with KCl while the slice was bathed in TTX-containing BBS. Outward currents were elicited in response to 40 ms step depolarizations applied from a holding potential of −60 mV to values ranging from −50 to +30 mV. The amplitude of the currents increased markedly with depolarization, as illustrated by the current–voltage relation plotted in Fig. 2*B*. These currents were characterized by a strong voltage dependence of their activation time course as well as by the lack of inactivation during the 40 ms pulses applied from −60 mV. As expected for currents flowing through K^+-selective channels, outward current tails were present upon return to the holding potential (the Nernst equilibrium potential for K^+ ions in this experiment was −95 mV). Moreover, these outward currents were greatly reduced when the cells were dialysed with CsCl pipettes (Fig. 1*A* and *C*). These currents correspond to the activation of voltage-gated K^+ channels. The fact that the K^+ currents shown in Fig. 2*A* did not inactivate is likely to be caused by the relatively depolarized holding potential used (−60 mV), a potential at which several types of K^+ channels are subject to slow inactivation (see Hille, 1992). When outward currents were elicited by depolarizing pulses applied from a holding potential of −90 mV they showed significant inactivation during 40 ms pulses (Fig. 2*C*). No attempt was made to further characterize the channel type(s) responsible for the outward currents.

Spontaneous synaptic input to stellate cells

Figure 3 illustrates another electrophysiological feature common to all the stellate cells examined in this study. When the voltage was held at −60 mV, spontaneous

inward current transients ranging in amplitude from 20 to 600 pA appeared at irregular intervals (Fig. 3*A*). The majority of the spontaneously occurring events were blocked by bath application of bicuculline (5 μM, Fig. 3*B*) and were therefore spontaneous synaptic inhibitory currents (IPSCs) mediated by the activation of

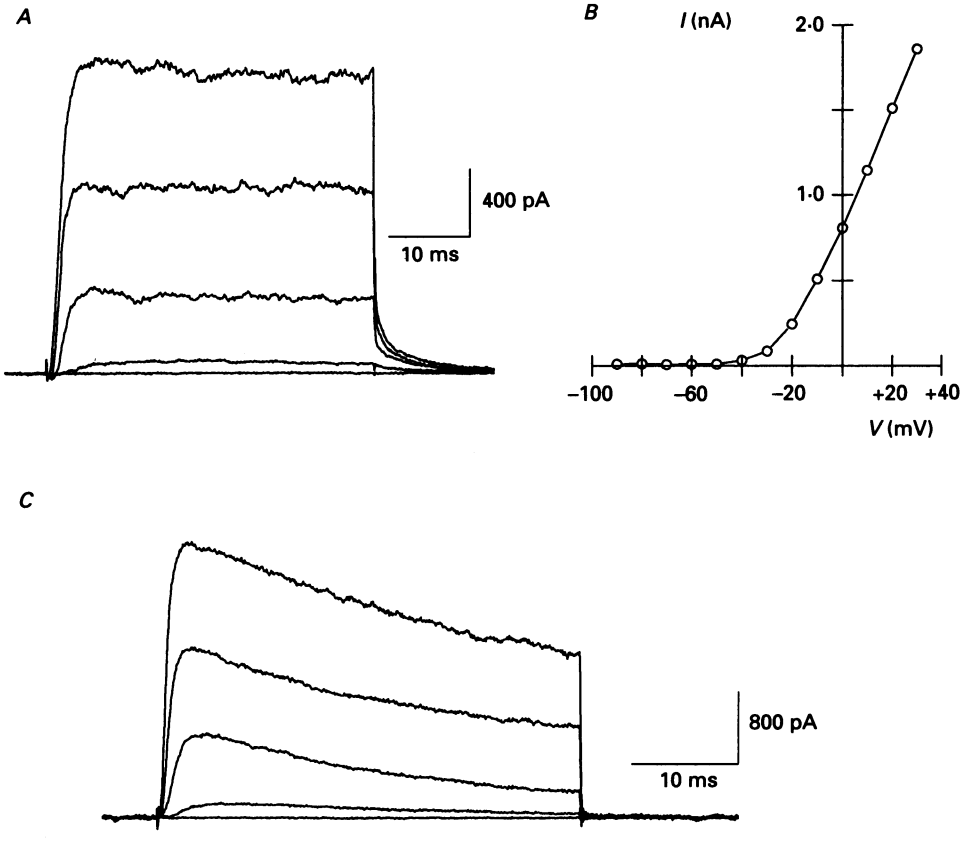

Fig. 2. Potassium currents in cerebellar stellate cells. *A*, whole-cell currents elicited by 40 ms depolarizing steps to values of −50, −30, −10, +10 and +30 mV. Holding potential, −60 mV. *B*, plot of the peak current *versus* the membrane voltage for the cell presented in *A*. *C*, outward currents elicited in another stellate cell held at a membrane potential of −90 mV, as the membrane was stepped to values of −60, −40, −20, 0 and +20 mV for 40 ms. In both cells the external solution was BBS with 0·5 μM TTX and the internal solution was KCl. In both *A* and *C*, leak currents and capacitative transients have been subtracted from the raw current records using appropriately scaled averaged current responses to 5 steps of −30 mV.

$GABA_A$ receptors. IPSCs were recorded as inward currents due to the Cl^- transmembrane gradient (see Methods); the value of E_{Cl} calculated from the Nernst equation is 0 mV. The time to peak of the IPSCs ($n = 81$) recorded from this cell was 1·1 ± 0·4 ms (mean ± S.D.). Most of the IPSCs decayed following a double exponential time course. A typical example of such events is shown on an expanded time scale in Fig. 3*C* (left trace). The continuous line superimposed on the experimental trace corresponds to the fit to the data of a double exponential function, with time

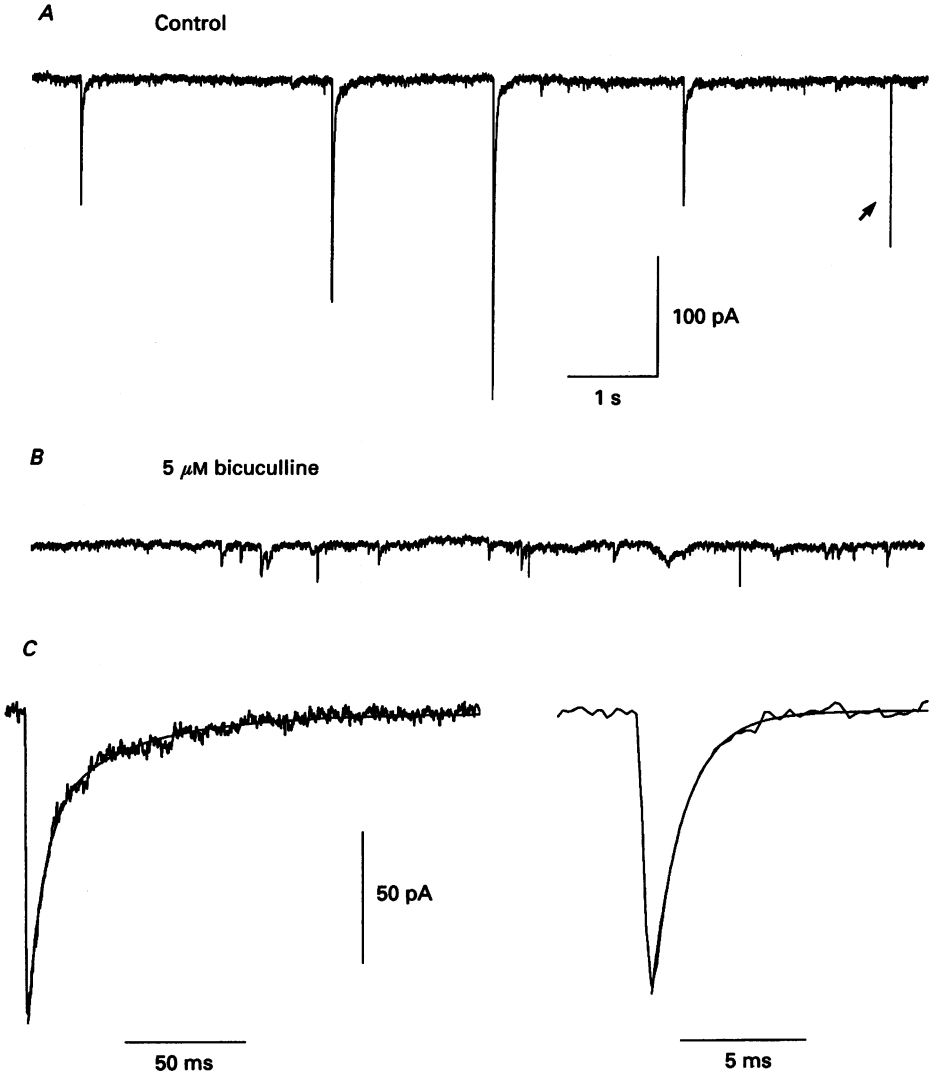

Fig. 3. Spontaneous synaptic currents in stellate cells. Samples of the continuous recording of spontaneous inward currents in a stellate cell, held at −60 mV in control saline (*A*) and after bath perfusion with 5 μM bicuculline (*B*). The arrow in *A* points to a 'fast' spontaneous synaptic event, characteristic of EPSCs. The traces in *C* show expanded views of the two types of spontaneous events recorded in control saline. The decay phase of the left trace, representative of GABAergic IPSCs, was best approximated by double exponential function with time constants of 6·6 and 37·2 ms (amplitude coefficients: −78 and −39 pA respectively). The decay of the right trace, representative of glutamatergic EPSCs, has been fitted with a single exponential function (time constant: 1·3 ms; amplitude coefficient, −107 pA). The fits are shown as continuous smooth traces superimposed on the experimental records.

constants of 6 and 37 ms. The mean values of the decay time constants (τ_1 and τ_2) for the IPSCs of this cell ($n = 81$) were 8 ± 3 ms and 36 ± 13 ms. The contribution of the slower component represented 43% of the peak current measured. Besides these

biphasic currents, a fraction of the bicuculline-sensitive inward synaptic currents (12% of the IPSCs analysed in this cell) had a decay phase that could be well approximated by a single exponential component (time constant of 14·8 ± 5·0 ms; 12 events).

TABLE 1. Parameters describing the time course of stellate cell IPSCs

Cell	Rise time (ms)	τ_1 (ms)	τ_2 (ms)	$A_2/(A_2+A_1)$	n
		Control			
a	1·1 ± 0·4	8·1 ± 3·6	35·7 ± 13·3	0·43 ± 0·12	81
b	1·2 ± 0·4	6·8 ± 2·1	33·0 ± 15·5	0·40 ± 0·17	105
c	1·2 ± 0·4	10·2 ± 2·7	46·0 ± 15·8	0·36 ± 0·14	125
d	1·3 ± 0·5	10·6 ± 4·1	50·4 ± 17·0	0·42 ± 0·15	100
e	0·9 ± 0·4	7·3 ± 2·1	30·0 ± 15·0	0·28 ± 0·11	114
f	1·2 ± 0·7	10·7 ± 5·0	56·0 ± 19·0	0·57 ± 0·16	191
g	1·0 ± 0·4	7·3 ± 2·4	35·1 ± 15·0	0·39 ± 0·14	196
Means ± S.E.M.	1·1 ± 0·1	8·7 ± 0·6	40·9 ± 3·7	0·41 ± 0·03	
		TTX			
g′	1·0 ± 0·3	9·1 ± 3·2	39·7 ± 14·8	0·42 ± 0·12	112
h	1·0 ± 0·3	6·8 ± 1·9	34·3 ± 13·7	0·28 ± 0·18	111
i	1·3 ± 0·5	11·2 ± 4·6	54·2 ± 20·0	0·52 ± 0·16	44
j	1·3 ± 0·4	7·7 ± 3·4	42·3 ± 18·6	0·40 ± 0·20	56
k	0·9 ± 0·3	9·1 ± 3·4	31·8 ± 14·7	0·25 ± 0·14	83
l	1·0 ± 0·3	10·7 ± 4·0	32·7 ± 15·6	0·41 ± 0·17	110
Means ± S.E.M.	1·1 ± 0·1	9·1 ± 0·7	39·2 ± 3·4	0·38 ± 0·04	

Rise times were calculated as the time from the baseline current level to the peak of the IPSC. The time constants of decay (τ_1 and τ_2) were obtained from the fit of the decay phase of individual IPSCs with a double exponential function. The relative contribution of the slow component was assessed as the ratio between its amplitude coefficient (A_2) and the sum of the two amplitude coefficients (A_2+A_1). IPSCs whose decay phase was well described by a single exponential function are not included in the table. Values for each cell are expressed as a mean ± standard deviation; n corresponds to the number of synaptic events analysed. IPSCs from cells a to g were recorded in normal BBS saline; IPSCs from cells g′ to l were recorded in the presence of 1 μM TTX.

Average mean values for the rise time and time constants of decay (τ_1 and τ_2) of IPSCs recorded from seven cells in control saline were 1·1 ± 0·1, 8·7 ± 0·6 and 40·9 ± 3·7 ms respectively (means ± S.E.M.). The average contribution of the second component to the decay phase of the current was 41%. The individual data for these parameters for each of the cells analysed is presented in Table 1 (cells a to g). In all the cells studied, no significant correlation was found between the amplitude of the IPSCs and their kinetic characteristics (rise time and decay time constants).

The frequency of occurrence of IPSCs recorded in control saline was quite variable from cell to cell. In twenty-one cells it ranged from 0·2 to 1·9 events per second (means ± S.E.M., 0·7 ± 0·1). The mean amplitude for the IPSCs in these twenty-one cells ranged from 61 to 226 pA (means ± S.E.M., 132 ± 11). Mean amplitude values, event frequency and the parameters describing the time course of IPSCs were quite stable in a given cell during whole-cell recording for durations up to 120 min.

In all stellate cells studied, a fraction (15–20%) of the spontaneous currents recorded in control saline exhibited kinetic properties distinct from those described above. These events were characterized by a fast activation and a rapid mono-

exponential decay (time to peak, 0·5±0·1 ms; time constant of decay, 1·3±0·2 ms; for twenty-two events analysed in the cell shown in Fig. 3). An example of this type of synaptic current is presented in Fig. 3*C* (right trace). The fit of the decay phase by a single exponential function with a time constant of 1·3 ms is displayed as a

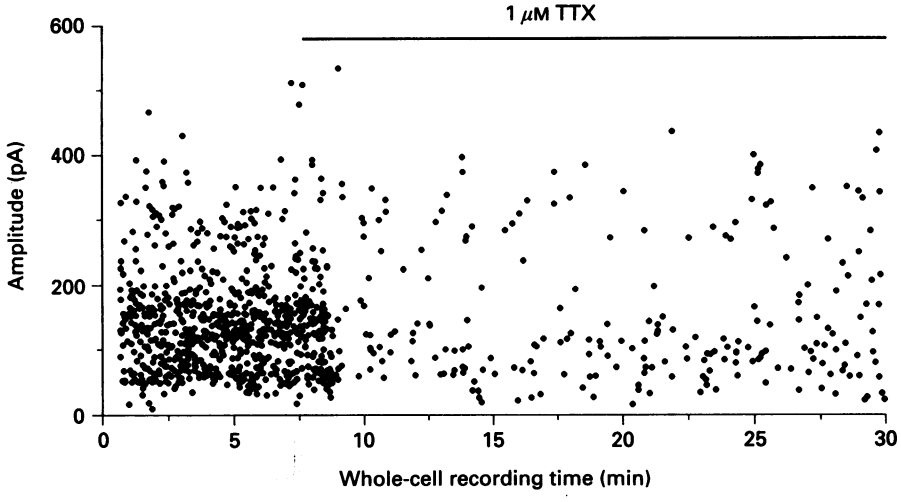

Fig. 4. Each point plots, as a function of time, the peak amplitude of individual IPSCs. Time 0 corresponds to the establishment of the whole-cell recording configuration. TTX was present in the bath solution during the time indicated by the bar above the plot. The mean amplitude±S.D. of the events was 143±79 in control saline and 149±87 pA in the presence of TTX.

continuous line superimposed on the experimental trace. Note the difference in time scale between the two traces of Fig. 3*C*. These 'fast' spontaneous events were eliminated by the addition of 5–10 μM CNQX to the bathing solution, which suggested that they were spontaneous excitatory glutamatergic postsynaptic currents.

Miniature IPSCs in stellate cells

Addition of TTX (1 μM) to the bathing solution had minimal effect on the amplitude or kinetics of the spontaneous IPSCs. The mean amplitude values of the IPSCs recorded in the presence of TTX were 141±13 pA (mean±S.E.M. for 22 cells). As discussed above, Na^+ currents of stellate cells were eliminated by TTX at concentrations of 0·1 μM. Thus, the dose used in the present experiments ensured a total block of Na^+ spikes in these cells and most likely in other neurones present in the slice. It was routinely checked, as shown by the insets in Fig. 5*A*, that the Na^+ currents were blocked from within the cell being recorded. The collection of synaptic events to be included in the amplitude histograms from TTX-treated cells was always started 2 min after the Na^+ currents in the recorded stellate cell were abolished.

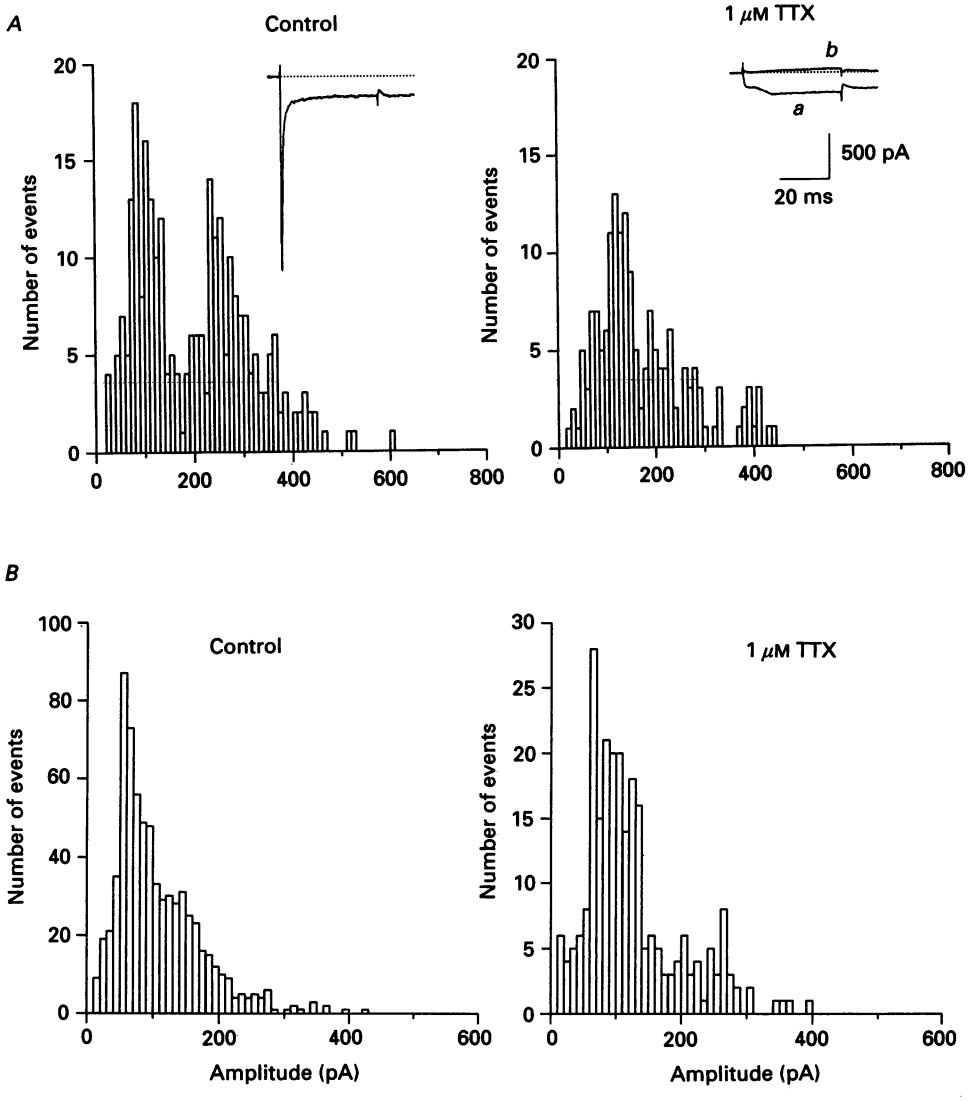

Fig. 5. Amplitude distributions of IPSCs and mIPSCs. Amplitude distributions for the IPSCs recorded from two different stellate cells in control saline (left) and in the presence of 1 μM TTX (right). In both experiments, sampling for the TTX histogram started when the voltage-gated Na^+ current was blocked. The inset in the left panel of *A* shows the inward current elicited in that cell by a 40 ms pulse to -20 mV in control saline. The inset in the right panel of *A* shows the inward current elicited by the same pulse 3 min after addition of TTX to the external saline (trace *a*). This residual inward current was later abolished by removal of external Ca^{2+} and addition of EGTA to the external solution (trace *b*). *A*, mean amplitude $\pm$ S.D. were 203 ± 112 pA for the control histogram (270 events) and 169 ± 92 for the TTX histogram (190 events). The recording period was the same in both cases (9 min). *B*, mean amplitude $\pm$ S.D. were 107 ± 64 pA for the control histogram (698 events) and 124 ± 72 for the TTX histogram (248 events). The recording periods were 6 min, control; 9·5 min, TTX.

A comparison of the amplitude distributions and event frequency in control saline and after the addition of TTX was carried out in twelve cells. It was found that the addition of TTX reduced to a variable extent the rate of occurrence of IPSCs. The ratio of IPSC frequency in TTX over that in control saline ranged from 0·11 to 0·92

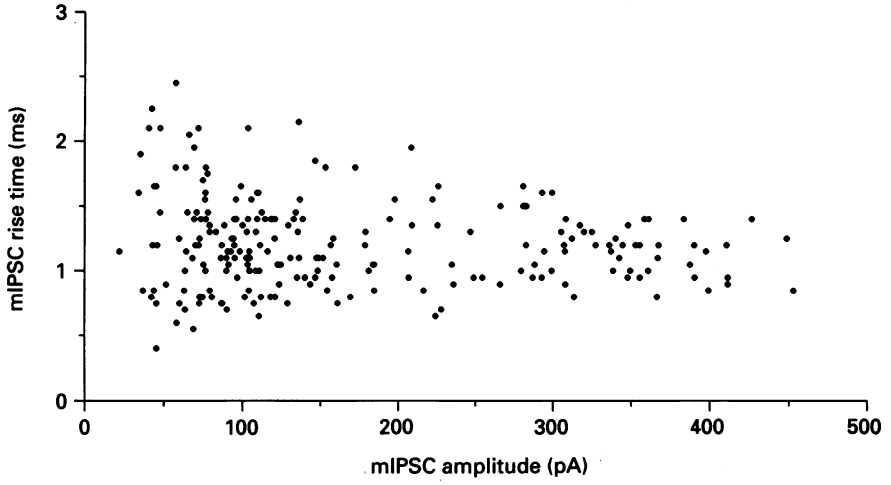

Fig. 6. Rise time of mIPSCs. Plot of the rise time of individual mIPSCs against their peak amplitude. The rise time was calculated as the difference in time between the first downward deflection from the baseline current and the peak of the current. mIPSCs were recorded in the presence of 1 μM TTX. They were filtered at 5 kHz and sampled at 50 μs per point.

(mean $\pm$ S.E.M., 0·47 $\pm$ 0·09; 12 cells). However, even in cells in which the frequency of events was drastically decreased by TTX, no systematic effect of the toxin was observed on the time course or on the amplitudes of IPSCs. Figure 4 plots the amplitude of individual synaptic events, as a function of time for an experiment in which the addition of TTX (1 μM) markedly reduced (by 89%) the frequency of IPSCs. It can be clearly seen that, in spite of the reduction in event frequency, there was no change in the amplitude of IPSCs even after bathing the slice in TTX for more than 20 min. The mean amplitude of the events was 143 $\pm$ 79 (790 events) in control saline and 149 $\pm$ 87 (209 events) in the presence of TTX.

A similar lack of effect of TTX on the mean amplitude values of IPSCs was observed in all twelve cells analysed. Examples of the amplitude distributions for two cells before and after addition of TTX are shown in Fig. 5. In the case of Fig. 5*A*, two distinct peaks were observed in control conditions, and a large fraction of the events in the second (larger amplitude) peak disappeared after the addition of TTX. As a result, the mean amplitude was slightly reduced in TTX (by 14%; see Fig. 5 legend). However, in some of the experiments in which two distinct peaks were present in the control histogram, it was the first (lower amplitude) peak which decreased in TTX, leading to a slight increase in IPSC mean amplitude. In other cells, such as that shown in Fig. 5*B*, the shape of the amplitude distributions was not significantly different before and after addition of TTX and the mean amplitude of the events in TTX was either similar or slightly higher than the control amplitude

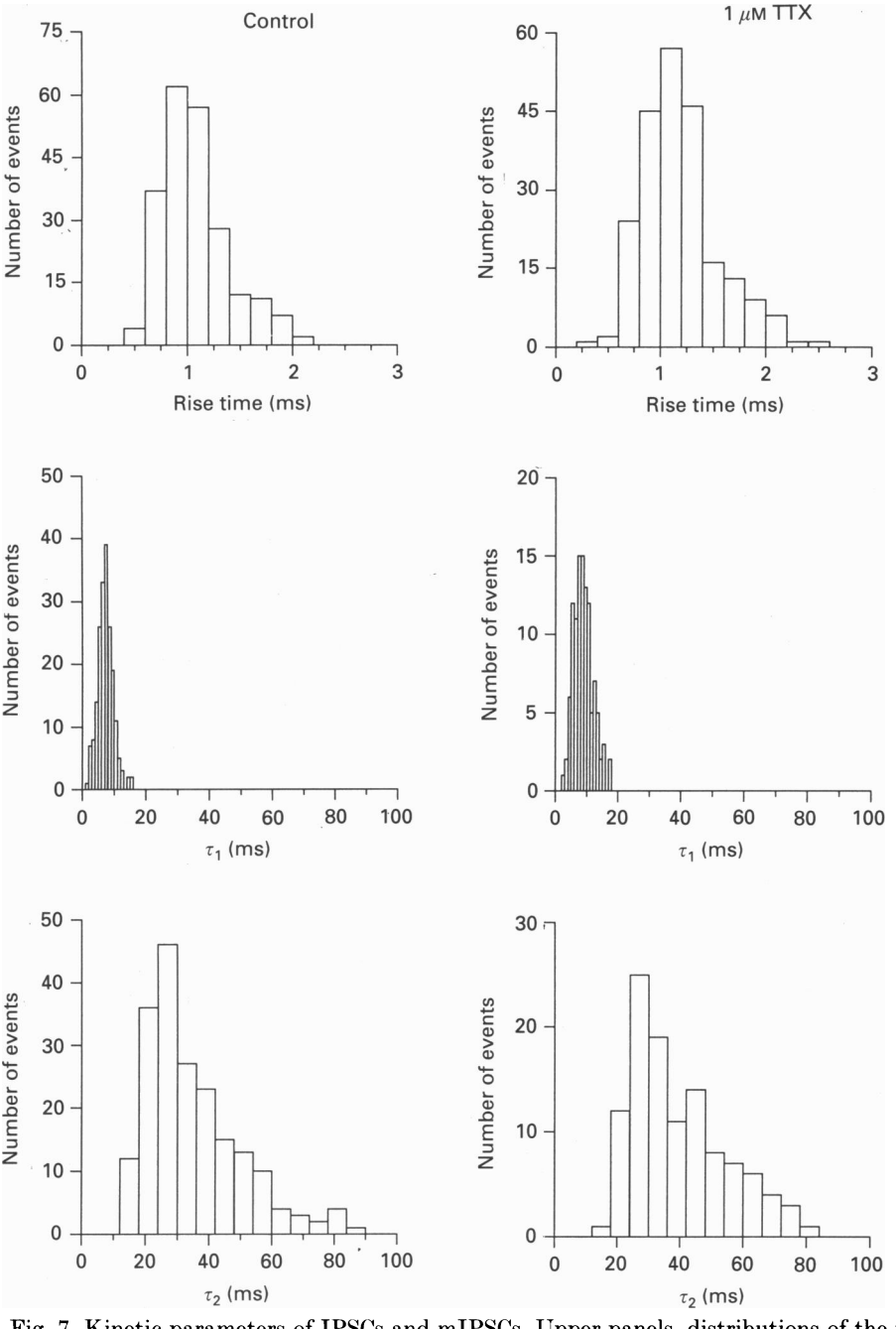

Fig. 7. Kinetic parameters of IPSCs and mIPSCs. Upper panels, distributions of the rise time of IPSCs. Middle and lower panels, distributions of the two time constants obtained from the fit of the decay phase of IPSCs with a double exponential function. The left panels present the distributions for the IPSCs recorded in control saline. The right panels show the corresponding distributions, for the same cell, in the presence of TTX. The mean values ± S.D. for each distribution are given in Table 1 (cell g for control; cell g′ for TTX). Same cell as in Fig. 6.

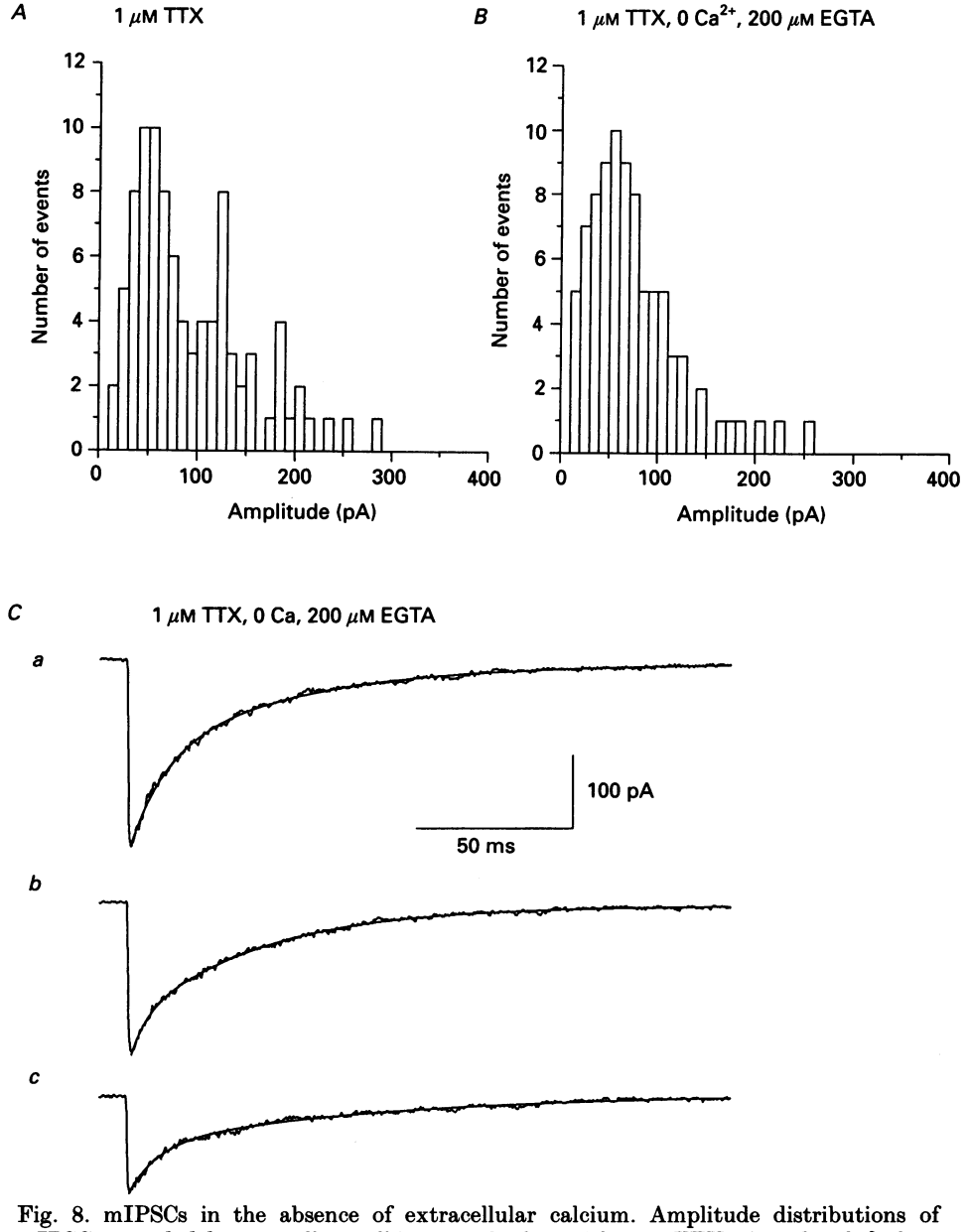

Fig. 8. mIPSCs in the absence of extracellular calcium. Amplitude distributions of mIPSCs recorded from a stellate cell in normal saline with 1 μM TTX (*A*) and in Ca^{2+}-free, TTX-containing saline supplemented with 200 μM EGTA and 2 mM $MgCl_2$ (*B*). Mean amplitude $\pm$ S.D. were 93 ± 58 pA for the TTX histogram (92 events) and 72 ± 41 pA for the Ca^{2+}-free saline histogram (85 events). The recording period is the same in both cases (9 min). Sampling for the Ca^{2+}-free saline histogram started 3 min after the bath solution had been exchanged, at which time the voltage-gated Ca^{2+} currents were abolished. *C*, examples of the IPSCs recorded from the same cell in Ca^{2+}-free saline. The decay phase of the currents has been fitted with double exponential functions. The fits are shown as continuous smooth traces superimposed on the experimental records. Fit parameters

(see legend for Fig. 5*B*). On average, the ratio of the mean amplitude in TTX over that in control saline was $1{\cdot}14 \pm 0{\cdot}10$ (12 cells). The average mean amplitude values of the synaptic events in the twelve cells were 134 ± 15 pA in control and 155 ± 22 pA in TTX. In all the cells studied, IPSCs with amplitudes larger than 100 pA were observed even after 30 min exposure to TTX.

Note that, even in TTX, the amplitude of IPSCs varies over a wide range, from 10 pA to several hundreds of picoamps. A possible explanation for the dispersion could be that the inputs which give rise to the synaptic events are located at different distances from the soma, and that the currents recorded are filtered to a variable extent depending on the location of the input. The amplitude of the synaptic events would then be expected to be positively correlated with their rise time. However, as in control conditions, the amplitude of single IPSCs recorded in TTX was independent of their rise time, as illustrated in Fig. 6. Other explanations that may account for the large dispersion of amplitudes of IPSCs will be addressed in the Discussion.

The parameters which characterize the time course of the IPSCs in TTX were found to be similar to those in TTX-free saline. Average mean values for the rise time and time constants of decay (τ_1 and τ_2) of IPSCs measured in six cells bathed in TTX saline were $1{\cdot}1 \pm 0{\cdot}1$, $9{\cdot}1 \pm 0{\cdot}7$ and $39{\cdot}2 \pm 3{\cdot}4$ ms respectively (means $\pm$ S.E.M.). The average contribution of the second component to the decay phase of the current was 38%. Table 1 (cells g′ to l) presents the individual data for these parameters for each of the cells analysed. The similarity of the kinetic characteristics of IPSCs before and after addition of TTX is further illustrated by Fig. 7. The left-hand columns correspond to distribution of the values of rise time (upper graph) and of the fast and slow time constants of decay of the IPSCs (middle and lower graphs respectively) in control condition. The columns on the right present the corresponding distributions for the IPSCs recorded in the same cell after addition of TTX (1 μM). The mean values of the distributions (see cell g and g′, Table 1) were similar in both conditions.

Given the lack of effect of TTX on the mean amplitude values of IPSCs, the possibility was considered that they resulted from synchronized multiquantal release of transmitter due to the discharge of Ca^{2+} spikes in the presynaptic inhibitory neurons. Experiments were therefore conducted under conditions designed to eliminate Ca^{2+} influx through voltage-gated Ca^{2+} channels. Figure 8 compares the amplitude distribution of IPSCs from a 9 min recording in TTX-containing saline (Fig. 8*A*) with the distribution obtained in the same cell after changing the extracellular solution to a TTX-containing saline in which Ca^{2+} was removed, the $MgCl_2$ concentration was increased to 2 mM and 200 μM EGTA was added (Fig. 8*B*; recording time 9 min). As shown above (see Fig. 1*C* and inset of Fig. 5*A*), the latter conditions result in the complete disappearance of voltage-gated Ca^{2+} currents. Nonetheless, the frequency of events in this Ca^{2+}-free saline was the same as that observed in TTX Ca^{2+}-containing saline. The mean amplitude of the IPSCs was slightly reduced (by 23%) in the Ca^{2+}-free saline (see Fig. 8 legend). Figure 8*C*

(time constants and amplitude coefficients) for each of the traces are as follows. *Ca*, 11·6 and 49·4 ms, −125 and −124 pA; *Cb*, 4·9 ms and 39·7 ms, −48 and −157 pA; *Cc*, 9·2 and 77·8 ms, −64 and −72 pA.

presents some examples of the IPSCs recorded in the same cell in TTX Ca^{2+}-free saline. Superimposed on the traces are the fits of the decay phase of the current by a double exponential function. The time constants obtained from the fits (see Fig. 8 legend for fit parameters) were within the range of the values obtained for this cell in TTX-containing saline having a normal concentration of Ca^{2+} (see cell h, Table 1).

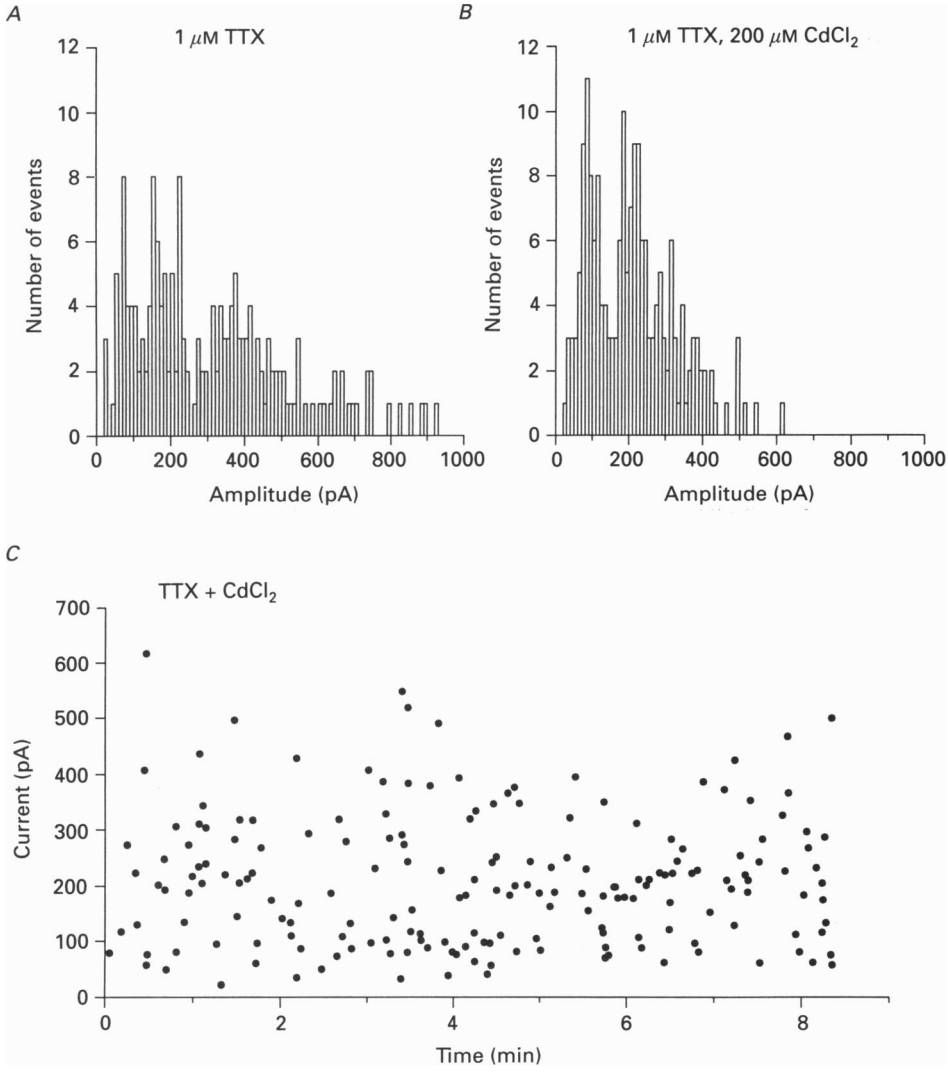

Fig. 9. mIPSCs in the presence of cadmium. Amplitude distributions of mIPSCs recorded in the presence of TTX (*A*) and after addition of 200 μM cadmium to the TTX saline (*B*). Mean amplitude $\pm$ S.D. were 313 ± 207 pA for the TTX histogram (177 events) and 207 ± 117 pA for the TTX + Cd^{2+} histogram (189 events). The recording period is the same in both cases (8·3 min). Sampling for the TTX + Cd^{2+} histogram started 2 min after the voltage-gated Ca^{2+} currents were blocked. *C*, plot of the amplitude of individual mIPSCs, recorded in the presence of TTX and cadmium, as a function of time. Data from the same cell as in *A* and *B*.

On average, neither the frequency of events, nor their mean amplitude was significantly affected by removal of extracellular Ca^{2+}. In four cells, IPSCs occurring in TTX Ca^{2+}-containing saline were compared with those observed in TTX Ca^{2+}-free, EGTA-containing saline in which concentration of $MgCl_2$ was raised (from 1 to

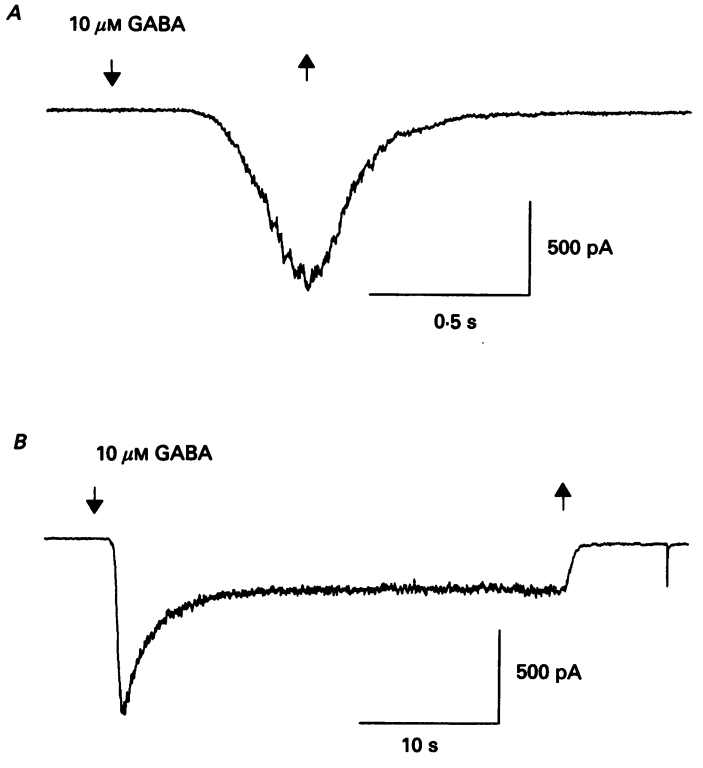

Fig. 10. Whole-cell GABA currents in stellate cells. *A*, inward current elicited in a stellate cell by a 0·6 s puff of 10 μM GABA during the time indicated by the arrows. *b*; response of the same cell to a longer application of GABA, time indicated by the arrows. Both the bath solution and the local puff solution contained 1 μM TTX.

2–5 mM). Changing to the Ca^{2+}-free solution reduced the mean frequency by 17 ± 20 % and the mean amplitude by 10 ± 5 %. As was the case with the TTX experiments, it was routinely checked that the Ca^{2+} currents in the recorded cell were abolished by the removal of Ca^{2+} or by the addition of Cd^{2+} (see below). The data collection for the histograms was started 2 min after the Ca^{2+} current was abolished.

Figure 9 shows data from one of three stellate cells in which Ca^{2+} influx was blocked by bathing the slice in a TTX-containing saline to which 200 μM $CdCl_2$ was added. The comparison of the amplitude distribution obtained in TTX-containing saline (Fig. 9*A*) with that obtained after addition of Cd^{2+} (Fig. 9*B*) shows that the Ca^{2+} channel blocker led to a 34 % decrease of the mean amplitude of IPSCs (see Fig. 9 legend), without changing the frequency of the synaptic events (recording time was the same in both histograms, i.e. 8·3 min). The plot of Fig. 9*C*, displays the amplitude of IPSCs recorded from this cell in the presence of Cd^{2+}–TTX-containing saline as a

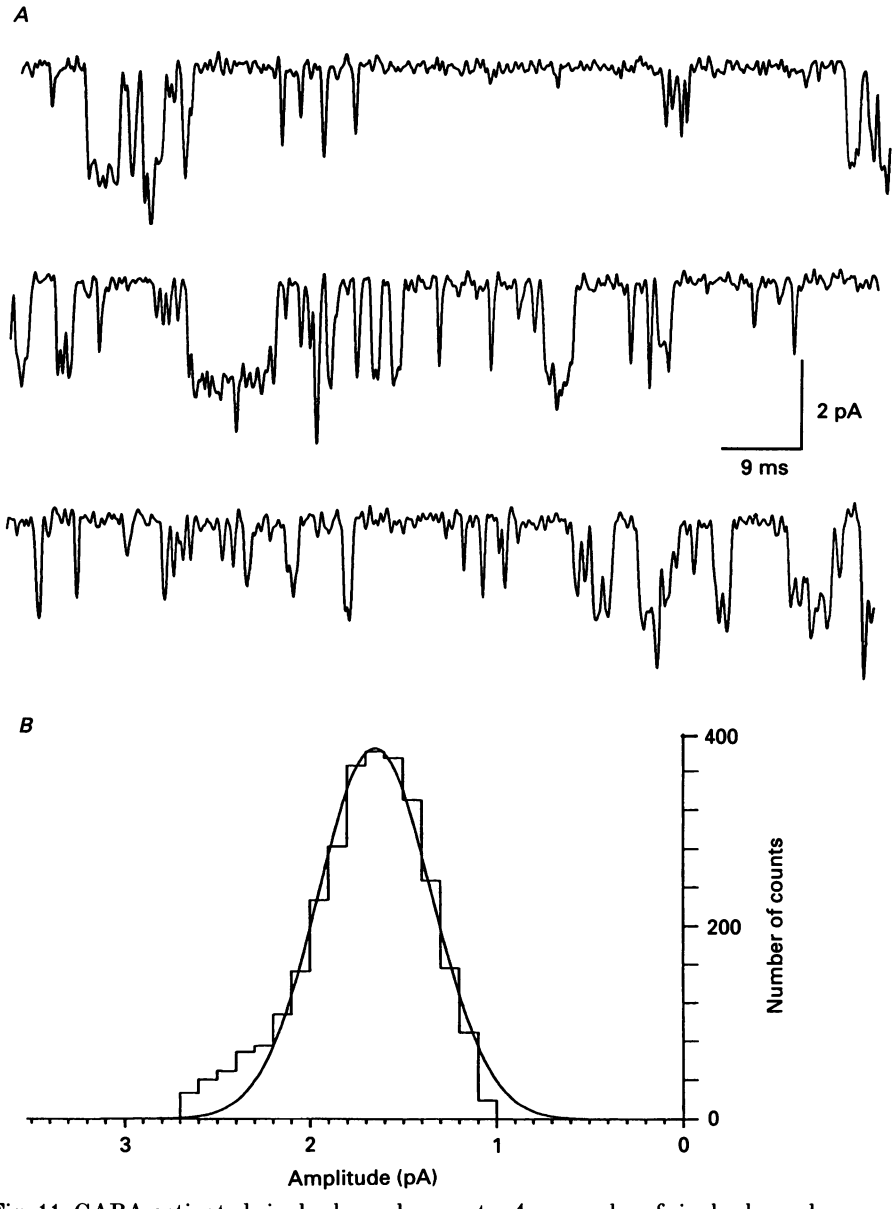

Fig. 11. GABA-activated single channel currents. *A*, examples of single channels currents recorded at −80 mV from an outside-out patch excised from the soma of a stellate cell. *B*, amplitude distribution of GABA-activated channels recorded from a different outside-out patch, held at a potential of −60 mV. The distribution has been fitted with a Gaussian function, with mean amplitude and S.D. of 1·64 and 0·34 pA, respectively. In both experiments, GABA was bath applied at a concentration of 1 μM. Data were sampled at 100 μs per point and filtered at 2 kHz.

function of time. The plot starts 2 min after the Ca^{2+} currents in the cell were abolished. Note that IPSCs of large amplitudes (200–600 pA) were still present even 10 min after complete block of the Ca^{2+} currents. A decrease in mean amplitude in

the presence of Cd^{2+} was observed in the three cells studied (average ratio for the mean amplitude of the events in TTX + Cd^{2+} to that in TTX was $0{\cdot}60 \pm 0{\cdot}12$). An interpretation of this effect could be that it results from a direct block of the postsynaptic $GABA_A$ receptors. Such an effect has been reported for Cd^{2+} and other divalent cations on GABA-induced currents of retinal cones (Kaneko & Tachibana, 1986).

$GABA_A$ receptor responses

Figure 10 shows the whole-cell currents elicited by local applications of GABA to a stellate cell in symmetrical Cl^- conditions. In the upper recording a 0·6 s puff-application of GABA (10 μM), during the time indicated by the arrows, led to an inward current associated with an increase in noise. The lower trace shows the current obtained from the same cell when the agonist was applied for a longer time (as indicated by the arrows; note the difference in time scale with the upper trace). Under these conditions, following the initial phase of inward current elicited by the amino acid, the response decreased to 25% of its peak value within 7 s. The non-desensitized portion of the agonist-induced current was associated with an increased noise level, and remained constant while the agonist was present. The GABA-induced responses were blocked by bath application of bicuculline (not shown).

Outside-out patches obtained from the somata of stellate cells presented a relatively high density of GABA-activated channels. In four outside-out patches, the application of GABA (10 μM) induced inward currents with peak amplitudes of 100–200 pA, which as in the whole-cell responses, rapidly decayed to a low current level in the continued presence of the amino acid.

In two outside-out patches in which lower concentrations of GABA (1 μM) were applied, single channel events were clearly resolved. Figure 11*A* shows selected portions of single current events elicited by GABA from a patch held at a potential of −80 mV. The amplitude of the elementary currents measured for the longer channel openings varied between 2·2 and 2·5 pA corresponding to a single channel chord conductance (γ) of about 28 pS. Figure 11*B* shows a histogram of the elementary current amplitudes for the GABA-activated channels of another patch held at a potential of −60 mV. The continuous line corresponds to the fit to the data of a single Gaussian function with a mean value for the single channel current of $1{\cdot}64 \pm 0{\cdot}34$ pA (mean ± S.D.). The corresponding value for γ was 27 pS. In two of the patches exposed to 10 μM GABA, single channel events could be detected on the desensitized phase of the response. Although a detailed analysis of these events was not carried out, the value of the single channel current in these cases was within the range of that of the events measured in the two patches exposed to lower GABA concentrations.

DISCUSSION

Stellate cell identification

Two main arguments support the identification of the cells studied in this paper as stellate cells: (a) their size, morphology and localization in the two outer thirds of the molecular layer of the cerebellar cortex, and (b) their neuronal character as shown by both the extracellular recording of spontaneous action potentials before

rupturing the membrane patch, and the appearance of spontaneous EPSCs and IPSCs when whole cell voltage-clamp recording was established. Although glial cells, especially in culture, may express voltage-dependent Na^+ and Ca^{2+} channels (see review Barres, Chun & Corey, 1990), the fact that the glial cells are endowed with large K^+ conductances (see Kuffler, 1967; Barres *et al.* 1990) makes it highly unlikely that they would discharge action potentials in brain slices bathed in normal saline. Furthermore, the occurrence of spontaneous synaptic currents is exclusive to neurons; these have never been reported in glial cells from either *in vivo* or *in vitro* preparations.

Other cerebellar inhibitory interneurons, the basket cells, are located closer to the Purkinje cell layer. Basket and stellate cells receive similar synaptic inputs: their main excitatory input comes from parallel fibres and their main inhibitory input from other basket and stellate cells (Ramón y Cajal, 1911; Lemkey-Johnston & Larramendi, 1968; Palay & Chan-Palay, 1974). Moreover, both inhibitory neurons are GABAergic (see Oertel *et al.* 1992) and the principal targets of their axons are the Purkinje cells. A difference between basket and stellate cells is that some of the basket cells may receive a GABAergic inhibitory input from collaterals of Purkinje axons (Ramón y Cajal, 1911; Mugnaini, 1972; O'Donoghue, King & Bishop, 1989). Given that stellate and basket cells share a common input, it is likely that some of the properties of synaptic currents in basket cells are similar to those of the stellate cells described here.

Excitatory synaptic currents in stellate cells

A small fraction of the spontaneous synaptic events recorded in the stellate cells were faster in onset and decay than the IPSCs and were blocked by CNQX. These were interpreted as being EPSCs mediated by the activation of non-NMDA glutamate receptors. Their time course of decay (time constants 1–1·3 ms) is similar to that of CNQX sensitive EPSCs from rat brain septal neurons (Schneggenburger, Lopez-Barneo & Konnerth, 1992) as well as of the fast, CNQX-sensitive component of the EPSCs in cerebellar granule cells (Silver, Traynelis & Cull-Candy, 1992). It is, in contrast, much faster than the EPSCs obtained from other central neurons with the same techniques and at the same temperature (see review in Table 1 of Schneggenburger *et al.* 1992). These EPSCs result from transmitter release at the synapses between parallel fibres and stellate cells (Eccles *et al.* 1966*a*, *b*; Chan-Palay & Palay, 1972; Palay & Chan-Palay, 1974).

Nature of the IPSCs

As already noted, stellate cells received inhibitory inputs from basket cells and other stellate cells. These inputs are presumably responsible for the spontaneous inhibitory synaptic currents described in the present study.

The spontaneously occurring IPSCs recorded from stellate cells were characterized by a fast rise time and a slow decay phase. The latter was described by a double exponential function, the slower time constant having values in the range of 30–50 ms. These features are shared by the GABAergic synaptic currents (spontaneous IPSCs and evoked IPSCs) recorded from granule cells in hippocampal slices (Edwards, Konnerth & Sakmann, 1990). In contrast, spontaneous and evoked

IPSCs in Purkinje cells exhibit a quite different time course, their decay phase being well approximated by a single exponential with a time constant in the range of 7–13 ms (Vincent, Armstrong and Marty, 1992). Interestingly, a minor fraction of the IPSCs in stellate cells had mono-exponential decays with time constants in the order of 12 ms. At present, it is impossible to know which mechanism(s) underlies these differences in kinetics of cerebellar IPSCs.

An interesting finding of our study was that in all stellate cells tested, IPSCs of large amplitude were observed in the presence of TTX at a concentration which completely abolishes their Na^+ current. One hypothesis which may be suggested to account for the relatively large amplitude TTX-resistant IPSCs would be that TTX does not penetrate the deeper levels of the thin cerebellar slices. It is, however, difficult to believe that the long exposure times (up to 20–30 min) used in these experiments are not sufficient to reach all the cells in the slice, since in the recorded stellate cell the Na^+ currents were blocked within 1 or 2 min of addition of the blocker. An alternative explanation would be that in the TTX-treated slices the IPSCs result from Ca^{2+}-dependent spikes that would release GABA from the synaptic terminals of the interneurons. This possibility is excluded by the fact that a large fraction of the large TTX-resistant IPSCs remained in Ca^{2+}-free saline or in the presence of Cd^{2+} ions.

Therefore, it appears that large IPSCs remain in the absence of any regenerative signal in presynaptic terminals. On the basis of the usual criteria for defining miniature synaptic currents (see Katz, 1969; Korn & Faber 1991) these spontaneous inhibitory currents may be called miniature IPSCs, i.e. they probably reflect the release of a single vesicle of transmitter. The mean amplitude of the miniature IPSCs is about ten times larger than the corresponding values found in hippocampal granule cells (Edwards *et al.* 1990) or in pyramidal cells (Ropert, Miles & Korn, 1991). The estimate of single channel conductance that was obtained from outside-out patches (27 pS) is within the range of the main conductance state of the GABA channel from other neurons (Bormann, Hamill & Sakmann, 1987; Edwards *et al.* 1990). Therefore, it is the number of GABA-gated channels activated during a miniature event that is particularly large in stellate cells. Thus, the largest mIPSCs recorded from these cells in the presence of TTX would result from the opening of at least 200 channels (*versus* 30 channels per mIPSC in hippocampal granule cells as reported by Edwards *et al.* 1990).

The amplitude of single quantal events in stellate cells varies over a wide range, from 20 to 400 pA, indicating large variations in the number of postsynaptic channels activated at different release sites. It is remarkable that the mean quantal size corresponds roughly to a tenfold increase of the resting conductance of stellate cells as measured with K^+-containing pipette solutions. This indicates that the spontaneous occurrence of a single quantal event will transiently clamp the cell potential close to E_{Cl} and prevent spontaneous firing and also presumably firing elicited by the excitatory inputs impinging upon stellate cells, for a period of time of around 20 ms.

In certain stellate cells (e.g. cell illustrated in Fig. 5*A*), histograms of unitary IPSCs obtained under control conditions (without TTX) displayed two peaks. In such experiments one of the peaks often disappeared after addition of TTX.

However, there was no simple integer ratio between the amplitude values of the multipeak histograms. This suggests that the peaks were not generated by multiquantal events. Furthermore, in some experiments, it was the low amplitude peak which was eliminated by TTX. To account for these observations we propose that multipeak histograms are generated by the activation of different release sites, each having a characteristic IPSC amplitude and action potential frequency, thus giving rise to the differential effects of TTX at the various release sites. On average, TTX did not modify the mean size of the IPSCs, while the frequency was often significantly decreased. This suggests that IPSCs resulting from presynaptic action potentials had amplitudes similar or identical to those of mIPSCs. A similar situation (but with a much smaller size of miniature EPSCs) is found in excitatory synapses of the rat hippocampus, where unitary excitatory synaptic currents have similar amplitudes in control saline and in TTX (Manabe, Renner & Nicoll, 1992; Raastad, Storm & Andersen, 1992). Our results suggest that in stellate cells spontaneous IPSCs result from the liberation of one, or occasionally two, quanta of GABA. The accompanying paper (Llano & Gerschenfeld, 1993) illustrates the changes brought about in this system under conditions of increased transmitter release.

Note added in proof. After submission of the revised version of this paper, two articles dealing with the properties of stellate cells in the turtle cerebellum were published: Mitgaard, J. (1992). Membrane properties and synaptic responses of Golgi cells and stellate cells in the turtle cerebellum *in vitro*. *Journal of Physiology* **457**, 329–354; and Mitgaard, J. (1992). Stellate cell inhibition of Purkinje cells in the turtle cerebellum *in vitro*. *Journal of Physiology* **457**, 355–367.

We thank Dr A. Marty for his advice and encouragement throughout the course of this work and for his comments on the manuscript. We are grateful to Drs P. Ascher, B. Barbour, H. Korn and C. Sotelo for helpful discussions and to Dr S. F. Traynelis and Mr Pierre Vincent for the programs used for analysis of synaptic activity. This work was supported by the Centre National de la Recherche Scientifique, France (URA 295) and by grant no. SC1*-CT91-0652 (TSTS) from the European Community.

REFERENCES

ALTMANN, J. (1972*a*). Postnatal development of the cerebellar cortex of the rat. I. The external germinal layer and the transitional molecular layer. *Journal of Comparative Neurology* **145**, 353–398.

ALTMANN, J. (1972*b*). Postnatal development of the cerebellar cortex in the rat. II. Phases in the maturation of Purkinje cells and of the molecular layer. *Journal of Comparative Neurology* **145**, 399–464.

ALTMANN, J. (1976). Experimental reorganization of the cerebellar cortex. VII. Effects of late irradiation that interfere with cell acquisition after stellate cells are formed. *Journal of Comparative Neurology* **165**, 65–76.

BARRES, B. A., CHUN, L. L. Y. & COREY, D. (1990). Ion channels in vertebrate glia. *Annual Review of Neuroscience* **13**, 441–474.

BORMANN, J., HAMILL, O. P. & SAKMANN, B. (1987). Mechanism of anion permeation through channels gated by glycine and γ-aminobutyric acid in mouse cultured spinal neurons. *Journal of Physiology* **385**, 243–286.

CHAN-PALAY, V. & PALAY, S. L. (1972). The stellate cells of the rat cerebellar cortex. *Zeitschrift für Anatomie und Entwicklungsgeschichte* **136**, 224–248.

ECCLES, J. C., LLINÁS, R. & SASAKI, K. (1966*a*). The inhibitory interneurons within the cerebellar cortex. *Experimental Brain Research* **1**, 1–16.

ECCLES, J. C., LLINÁS, R. & SASAKI, K. (1966*b*). Parallel fiber stimulation and the responses induced thereby in the Purkinje cells of the cerebellum. *Experimental Brain Research* **1**, 17–39.

EDWARDS, F. A., KONNERTH, A., SAKMANN, B. & TAKAHASHI, T. (1989). A thin slice preparation for patch-clamp recordings from neurones of the mammalian central nervous system. *Pflügers Archiv* **414**, 600–612.

EDWARDS, F. A., KONNERTH, A. & SAKMANN, B. (1990). Quantal analysis of inhibitory synaptic transmission in the dentate gyrus of rat hippocampal slices: a patch-clamp study. *Journal of Physiology* **430**, 213–249.

HAMILL, O. P., MARTY, A., NEHER, E., SAKMANN, B. & SIGWORTH, F. (1981). Improved patch-clamp techniques for high-resolution current recording from cells and cell-free membrane patches. *Pflügers Archiv* **391**, 85–100.

HILLE, B. (1992). *Ionic Channels of Excitable Membranes*, 2nd edition. Sinauer Associates Inc. Sunderland, MA, USA.

HILLMAN, D. E. (1969). Neuronal organization of the cerebellar cortex in amphibia and reptilia. In *Neurobiology of Cerebellar Evolution and Development*, ed. LLINÁS, R., pp. 279–324. American Medical Association Education and Research Foundation, Chicago.

HÖKFELT, T. & LJUNGDAHL, Å. (1972). Autoradiographic identification of central and cerebellar cortical neurones accumulating labelled gamma-aminobutyric acid (^{3}H-GABA). *Experimental Brain Research* **14**, 354–362.

KANEKO, A. & TACHIBANA, M. (1986). Blocking effects of cobalt and related ions on the γ-aminobutyric acid-induced current in turtle retinal cones. *Journal of Physiology* **373**, 463–479.

KATZ, B. (1969). *The Release of Neural Transmitter Substances*. Charles C. Thomas, Springfield, IL, USA.

KORN, H. & FABER, D. S. (1991). Quantal analysis and synaptic efficacy in the CNS. *Trends in Neurosciences* **14**, 439–445.

KRISHTAL, O. A. & PIDOPLICHKO, V. I. (1980). A receptor for protons in the nerve cell membrane. *Neuroscience* **5**, 2325–2327.

KUFFLER, S. W. (1967). The Ferrier Lecture. Physiological Properties and a potassium-mediated effect of neuronal activity on glial membrane potential. *Proceedings of the Royal Society* B **168**, 1–21.

LEMKEY-JOHNSTON, N. & LARRAMENDI, L. M. H. (1968). Types and distribution of synapses upon basket and stellate cells of the mouse cerebellum: an electron-microscopy study. *Journal of Comparative Neurology* **134**, 73–112.

LLANO, I. & GERSCHENFELD, H. M. (1991). Cerebellar stellate neurons: a microphysiological and pharmacological study. *European Journal of Neuroscience* **3**, suppl. 3, 300.

LLANO, I. & GERSCHENFELD, H. M. (1993). β-Adrenergic enhancement of inhibitory synaptic activity in rat cerebellar stellate and Purkinje cells. *Journal of Physiology* **468**, 201–224.

LLANO, I., LERESCHE, N. & MARTY, A. (1991*a*). Calcium entry increases the sensitivity of cerebellar Purkinje cells to applied GABA and decreases inhibitory synaptic currents. *Neuron* **6**, 565–574.

LLANO, I., MARTY, A., ARMSTRONG, C. M. & KONNERTH, A. M. (1991*b*). Synaptic- and agonist-induced excitatory currents of Purkinje cells in rat cerebellar slices. *Journal of Physiology* **434**, 183–213.

LLINÁS, R. (1969). Functional aspects of interneuronal evolution in the cerebellar cortex. In *The Interneuron*, ed. BRAZIER, M. A., pp. 329–348. University of California Press, Los Angeles.

LLINÁS, R. & SUGIMORI, M. (1980). Electrophysiological properties of *in vitro* Purkinje cell somata in mammalian cerebellar slices. *Journal of Physiology* **305**, 171–195.

MANABE, T., RENNER, P. & NICOLL, R. A. (1992). Postsynaptic contribution to long-term potentiation revealed by the analysis of miniature synaptic currents. *Nature* **355**, 50–55.

MUGNAINI, E. (1972). The histology and cytology of the cerebellar cortex. In *The Comparative Anatomy of the Cerebellum. The Human Cerebellum, Cerebellar Connections and Cerebellar Cortex*, ed. LARSELL, O. & JANSEN, J., pp. 201–264. University of Minnesota, Minneapolis, MN, USA.

O'DONOGHUE, D. L., KING, J. S. & BISHOP, G. A. (1989). Physiological and anatomical studies of the interactions between Purkinje cells and basket cells in the cat's cerebellar cortex. Evidence for a unitary relationship. *Journal of Neurosciences* **9**, 2141–2150.

OERTEL, W. H., MUGNAINI, E., SCHEMECHEL, D. E., TAPPAZ, M. L. & KOPIN, I. J. (1982). The immunochemical demonstration of GABAergic neurons – methods and applications. In *Cytochemical Methods in Neuroanatomy*, ed. CHAN-PALAY, V. & PALAY, S. L., pp. 297–329. Alan R. Liss, New York.

PALAY, S. L. & CHAN-PALAY, V. (1974). *Cerebellar Cortex: Cytology and Organization*. Springer, Berlin.

PALKOVITS, M., MAGYAR, P. & SZENTÁGOTHAI, J. (1971). Quantitative histological analysis of the cerebellar cortex in the cat. III. Structural organization of the molecular layer. *Brain Research* **34**, 1–18.

RAASTAD, M., STORM, J. F. & ANDERSEN, P. (1992). Putative single quantum and single fibre excitatory postsynaptic currents show similar amplitude range and variability in rat hippocampal slices. *European Journal of Neuroscience* **4**, 113–117.

RAMON Y CAJAL, S. (1911). *Histologie du Système Nerveux d l'Homme et des Vertebrés*. Consejo Nacional de Investigacions Científicas, Madrid (Reprinted 1955).

RAMON Y CAJAL, S. (1888). Estructura de los centros nerviosos de las aves. *Revista Trimestral de Histología Normal y Patológica* No. 1. Reprinted (1924) in *Trabajos Escogidos*, vol. 1, pp. 305–315. Jiménez y Molina, Madrid.

ROPERT, N., MILES, R. & KORN, H. (1991). Characteristics of miniature postsynaptic currents in CA1 pyramidal neurones of rat hippocampus. *Journal of Physiology* **428**, 707–722.

SCHNEGGENBURGER, R., LÓPEZ BARNEO, J. & KONNERTH, A. (1992). Excitatory and inhibitory synaptic currents and receptors in rat medial septal neurons. *Journal of Physiology* **445**, 261–276.

SCHON, F. & IVERSEN, L. L. (1972). Selective accumulation of ^{3}[H]-GABA by stellate cells in rat cerebellar cortex *in vivo*. *Brain Research* **42**, 503–507.

SILVER, R. A., TRAYNELIS, S. F. & CULL-CANDY, S. G. (1992). Rapid-time-course miniature and evoked excitatory currents at cerebellar synapses *in situ*. *Nature* **355**, 163–166.

VINCENT, P., ARMSTRONG, C. M. & MARTY, A. (1992). Inhibitory synaptic currents in cat cerebellar cells: modulation by postsynaptic depolarisation. *Journal of Physiology* **456**, 453–471.